Journal of Statistical Mechanics:
Theory and Experiment

PAPER: CLASSICAL STATISTICAL MECHANICS, EQUILIBRIUM AND NON-EQUILIBRIUM

Irreversible and endoreversible behaviors of the LD-model for heat devices: the role of the time constraints and symmetries on the performance at maximum χ figure of merit

To cite this article: Julian Gonzalez-Ayala *et al J. Stat. Mech.* (2016) 073202

Journal of Statistical Mechanics: Theory and Experiment
An IOP and SISSA journal

PAPER: Classical statistical mechanics, equilibrium and non-equilibrium

Irreversible and endoreversible behaviors of the LD-model for heat devices: the role of the time constraints and symmetries on the performance at maximum χ figure of merit

Julian Gonzalez-Ayala[1], **A Calvo Hernández**[1] **and J M M Roco**[1,2]

[1] Departamento de Física Aplicada, Universidad de Salamanca, 37008 Salamanca, Spain
[2] Instituto Universitario de Física Fundamental y Matemáticas (IUFFyM), Universidad de Salamanca, 37008 Salamanca, Spain
E-mail: jgonzalezayala@usal.es

Received 19 April 2016
Accepted for publication 14 May 2016
Published 8 July 2016

Online at stacks.iop.org/JSTAT/2016/073202
doi:10.1088/1742-5468/2016/07/073202

Abstract. The main unified energetic properties of low dissipation heat engines and refrigerator engines allow for both endoreversible or irreversible configurations. This is accomplished by means of the constraints imposed on the characteristic global operation time or the contact times between the working system with the external heat baths and modulated by the dissipation symmetries. A suited unified figure of merit (which becomes power output for heat engines) is analyzed and the influence of the symmetries on the optimum performance discussed. The obtained results, independent on any heat transfer law, are faced with those obtained from Carnot-like heat models where specific heat transfer laws are needed. Thus, it is shown that only the inverse phenomenological law, often used in linear irreversible thermodynamics, correctly reproduces all optimized values for both the efficiency and coefficient of performance values.

Keywords: nonlinear dynamics, transport processes/heat transfer

1742-5468/16/073202+19$33.00

Contents

1. Introduction

A key requirement in the thermodynamic optimization of processes in finite time is to understand the limits of what can be achieved in such processes, as its implications on the use of energy resources in any operation of energy conversion. As noted by Salamon *et al* [1] there is much to be learned from the evaluation of unified models considering a host of possible loss mechanisms with a host of possible constraints and optimizing a host of possible objectives.

A paradigmatic unified model of heat devices is the so-called low dissipation (LD), first introduced by Esposito *et al* [2] for heat engines (HE), extended for refrigerator engines (RE) [3–7] and whose validity has been proven for a wide class of heat devices [8–13]. The core of the model is the assumption that entropy generation is assumed as inversely proportional to the time duration of the isothermal processes and modulated by generic dissipation factors (adiabatic processes are not considered at all) so that the reversible regime is recovered in the limit of infinite times. A significant consequence is the linking of the bounds for the efficiency and coefficient of performance to symmetry considerations but without reference to any specific heat transfer law. For this model, some of us [14] recently reported a study which has special emphasis on the irreversibilities associated not only to the total cycle time but also to the contact times of the working system with the external heat reservoirs and their influence on different optimization criteria for both HE and RE.

On the other side, entropy generation is, in last instance, the fundamental thermodynamic magnitude accounting for the unavoidable irreversibilities of real heat devices. The evaluation of this magnitude in a particular design requires a model linking the thermodynamic non-ideality of the design to the physical characteristics of the system.

J. Stat. Mech. (2016) 073202

In this context, LD models offer the possibility of explicit calculations of the entropy generation and then it is amenable for a deep analysis of how the main energetic properties of the device are affected by the different nature of irreversibilities. Our main goal in this paper is to analyze how irreversibilities accounted by the total cycle time, the external contact times, and the symmetries in the dissipations may yield irreversible or endoreversible configurations, which are further analyzed in light of the most standard Carnot-like irreversible models where specific heat transfer laws are required. In particular we stress the behavior of the performance at maximum figure of merit χ, an optimization criterion focused on the common characteristics of the energy converter instead of any particular coupling to the external heat bath and mathematically defined as $\chi = zQ_{\rm in}/t$, where z is the first-law thermal efficiency of the converter [3], and whose suitability for different heat devices has been reported in a number of recent papers [15–27]. New physical insights about the bounds of the efficiency and COP are obtained and discussed in terms of Carnot-like heat-transfer dependent models. After a brief theoretical summary, we present our results for heat engines and refrigerators separately.

2. Theoretical background

Here we stress the main conceptual aspects of the model concerning entropy generation, symmetries and time. Specific details can be found in [14]. This model considers that the entropy generation in the processes where heat exchanges between working systems and the hot and cold reservoirs (at temperatures $T_{\rm h}$ and $T_{\rm c}$, respectively) is inversely proportional to the time of the process $t_{\rm h}$ and $t_{\rm c}$,

$$\Delta S_{T_{\rm h}} = \mp \Delta S + \frac{\Sigma_{\rm h}}{t_{\rm h}}, \tag{1}$$

$$\Delta S_{T_{\rm c}} = \pm \Delta S + \frac{\Sigma_{\rm c}}{t_{\rm c}}, \tag{2}$$

where ΔS is the working system entropy change generated while in contact with the external reservoir and the parameters $\Sigma_{\rm h}$ and $\Sigma_{\rm c}$ contain information about how dissipation increases as one moves from the reversible limit, which is reached in the limits $t_{\rm h} \to \infty$ and $t_{\rm c} \to \infty$ (a Carnot engine operating between $T_{\rm h}$ and $T_{\rm c}$, the reversible engine baseline). The signs $\mp(\pm)$ in equation (1) (equation (2)) account for the opposite sense of the heat fluxes exchanged with the hot (cold) reservoir for HE and RE, respectively. The energies absorbed by the working fluid are assumed positive while the energies released by the working fluid are assumed to be negative. For a cycle, the total entropy $\Delta S_{\rm tot}$ will be determined by the sum of $\Delta S_{T_{\rm h}}$ and $\Delta S_{T_{\rm c}}$, given from equations (1) and (2):

$$\Delta S_{\rm tot} = \frac{\Sigma_{\rm h}}{t_{\rm h}} + \frac{\Sigma_{\rm c}}{t_{\rm c}}. \tag{3}$$

J. Stat. Mech. (2016) 073202

With the assumption of instantaneous adiabatic processes, the total time of the cycle is given by $t = t_{\rm h} + t_{\rm c}$, so that $\alpha \equiv t_{\rm c}/t$ and $1-\alpha \equiv t_{\rm h}/t$ define the fractional contact times with the cold and hot reservoirs, respectively. In a similar way, from a total dissipation parameter $\Sigma_{\rm T} \equiv \Sigma_{\rm h} + \Sigma_{\rm c}$, the relative dissipation to the external reservoirs are given by $\widetilde{\Sigma}_{\rm c} \equiv \Sigma_{\rm c}/\Sigma_{\rm T}$ and by $\widetilde{\Sigma}_{\rm h} \equiv \Sigma_{\rm h}/\Sigma_{\rm T} = 1-\widetilde{\Sigma}_{\rm c}$. With the above definitions equation (3) can be expressed in terms of t, α, $\Sigma_{\rm T}$ and $\widetilde{\Sigma}_{\rm c}$ in the form:

$$\Delta S_{\rm tot} = \Sigma_{\rm T}\left[\frac{1-\widetilde{\Sigma}_{\rm c}}{(1-\alpha)t} + \frac{\widetilde{\Sigma}_{\rm c}}{\alpha t}\right]. \tag{4}$$

Two notable characteristics of the model are the size and an appropriate dimensionless cycle time. Since ΔS is associated to the heat exchanges with the reservoirs in the baseline reversible machine, it can be considered as a measure of the size of the heat device and then we can define a relative size by the ratio $\Delta S_{\rm tot}/\Delta S$. Besides, since $\Sigma_{\rm T}/\Delta S$ has time units it defines a characteristic time scale as the ratio between dissipation parameter, $\Sigma_{\rm T}$, and the entropy exchange, ΔS. This allows us to define a characteristic dimensionless time $\tilde{t} \equiv (t\,\Delta S)/\Sigma_{\rm T}$, so that total cycle times $\tilde{t} \leqslant 1$ should correspond to working regimes with high dissipations, while working regimes with $\tilde{t} \gg 1$ are expected to describe efficient energy converters. In this way, the dimensionless total entropy generated per unit time is given by:

$$\widetilde{\dot{\Delta S}}_{\rm tot} \equiv \frac{\Delta S_{\rm tot}}{t}\,\frac{\Sigma_{\rm T}}{\Delta S^2} = \frac{1}{\tilde{t}}\left[\frac{1-\widetilde{\Sigma}_{\rm c}}{(1-\alpha)\tilde{t}} + \frac{\widetilde{\Sigma}_{\rm c}}{\alpha\tilde{t}}\right]. \tag{5}$$

A second unified magnitude is the figure of merit $\chi = zQ_{\rm in}/t$. It becomes power output P for HE and the COP (ϵ) times cooling rate (R) for refrigerators:

$$\chi^{\rm (HE)} = \frac{\eta\, Q_{\rm h}}{t_{\rm cycle}} = -\,\frac{W}{t_{\rm cycle}} = P, \tag{6}$$

$$\chi^{\rm (RE)} = \frac{\epsilon Q_{\rm c}}{t_{\rm cycle}} = \epsilon R. \tag{7}$$

In terms of dimensionless units the involved magnitudes in the above equations read as:

$$\widetilde{P} \equiv -\frac{W}{t}\,\frac{\Sigma_{\rm T}}{T_{\rm c}\Delta S^2} = \left[\frac{1}{\tau} - 1 - \frac{1}{\tau}\left(\frac{1-\widetilde{\Sigma}_{\rm c}}{(1-\alpha)\tilde{t}}\right) - \frac{\widetilde{\Sigma}_{\rm c}}{\alpha\tilde{t}}\right]\frac{1}{\tilde{t}}, \tag{8}$$

$$\widetilde{R} \equiv \widetilde{\dot{Q}}_{\rm c} \equiv \frac{Q_{\rm c}}{t}\,\frac{\Sigma_{\rm T}}{T_{\rm h}\Delta S^2} = \tau\left(1 - \frac{\widetilde{\Sigma}_{\rm c}}{\alpha\tilde{t}}\right)\frac{1}{\tilde{t}}, \tag{9}$$

$$\epsilon = \frac{\left(1-\frac{\widetilde{\Sigma}_{\rm c}}{\alpha\tilde{t}}\right)\tau}{1-\tau+\frac{1-\widetilde{\Sigma}_{\rm c}}{(1-\alpha)\tilde{t}} + \frac{\tau\widetilde{\Sigma}_{\rm c}}{\alpha\tilde{t}}}, \tag{10}$$

J. Stat. Mech. (2016) 073202

$$\widetilde{\chi} = \frac{\left(1 - \frac{\widetilde{\Sigma}_c}{\alpha \tilde{t}}\right)^2 \tau^2}{\left[1 - \tau + \frac{1 - \widetilde{\Sigma}_c}{(1-\alpha)\tilde{t}} + \frac{\tau \widetilde{\Sigma}_c}{\alpha \tilde{t}}\right] \tilde{t}}. \tag{11}$$

For simplicity, from now on $\widetilde{\chi}$ refers to $\widetilde{\chi}^{(\mathrm{RE})}$.

3. Results: heat engines

To begin with, we plot in figure 1 a 3D-plot of the efficiency, the dimensionless power output, and the dimensionless total entropy generation by the parametric elimination of α and $\tilde{t}$ for a symmetric dissipation $\widetilde{\Sigma}_c = 0.5 = \widetilde{\Sigma}_h$. Following the α-values for a fixed time cycle we can clearly observe the characteristic loops of real heat engines usually obtained by finite-time Carnot-like irreversible models with heat leak [28–33]. On the other hand, by following the $\tilde{t}$-values for fixed α it is possible to observe open, parabolic behaviors for the dimensionless power output versus efficiency which usually comes from endoreversible-like models where all irreversibilities are restricted to the coupling of the working system with the external heat baths [28–33]. These behaviors suggest that for a given total dimensionless cycle time, the variation of the contact time has implicit the role of an internal irreversibility, while by fixing the external contact times the variation of the total time of the cycle carries the role of an external irreversibility on it.

The explicit influence of the dissipation constant $\widetilde{\Sigma}_c$ is shown in the 2D-plots of figure 2; for a fixed cycle time, figures 2(a) and (b), and for fixed contact time α, figures 2(c) and (d). The characteristic loop of real heat engines in figure 2(a) (with near but non-coincident maximum power and maximum efficiency states) is clearly visible and confined by the monotonic behavior imposed by the limit values $\widetilde{\Sigma}_c \to 1$ ($\widetilde{\Sigma}_h \to 0$) and $\widetilde{\Sigma}_c \to 0$ ($\widetilde{\Sigma}_h \to 1$). Note how the entropy generation shows well defined minimum values close but non-coincident with the maximum values of the dimensionless power (nor with maximum efficiency) values (figure 2(b) and also in figure 1(b)). From equation (12) and equations (39)–(40) of [14] it is possible to see that the values of α that optimize each quantity are different. In figures 2(c) and (d) we observe a quite different behavior with well defined maxima values of power but monotonic increasing of both efficiency and entropy generation, respectively. A very clear consequence of the all the above results is that the equivalence or not of the maximum power, maximum efficiency and minimum entropy performance regimes depend on the constraints imposed on the model [1].

In particular, of special relevance in the optimization of energy conversion processes in heat engines is the regime of maximum power and the corresponding efficiency, which has been widely analyzed in many different contexts for both isolated [34–52] and coupled heat engines [53–55]. A key result of the LD-model for HE is that power output can be optimized for both the characteristic total cycle time $\tilde{t}$ and for the fractional contact times with the external heat baths α [14]. The values of $\tilde{t}$ and α giving maximum power are:

J. Stat. Mech. (2016) 073202

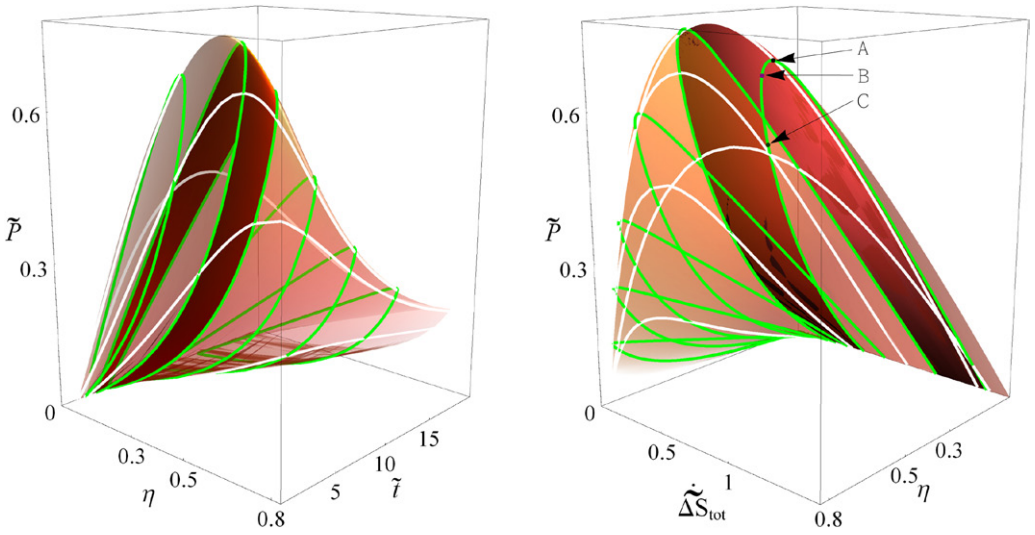

Figure 1. (a) Evolution of η-$\widetilde{P}$ with respect to $\tilde{t}$. (b) Evolution of η-$\widetilde{P}$ (with maxima at B and A, respectively for the curve with $\tilde{t}=2$) with respect to $\dot{\widetilde{\Delta S}}_{\rm tot}$ (with minimum at C). In both cases green lines correspond to $\tilde{t}=$ const. and $\alpha\in(0,1)$ and white lines to $\alpha=$ const. and $\tilde{t}\in(0,20)$. Note the loop-like behavior of the green curves and the open parabolic of the white ones. In all cases $\tau=0.2$, $\eta_C=0.8$.

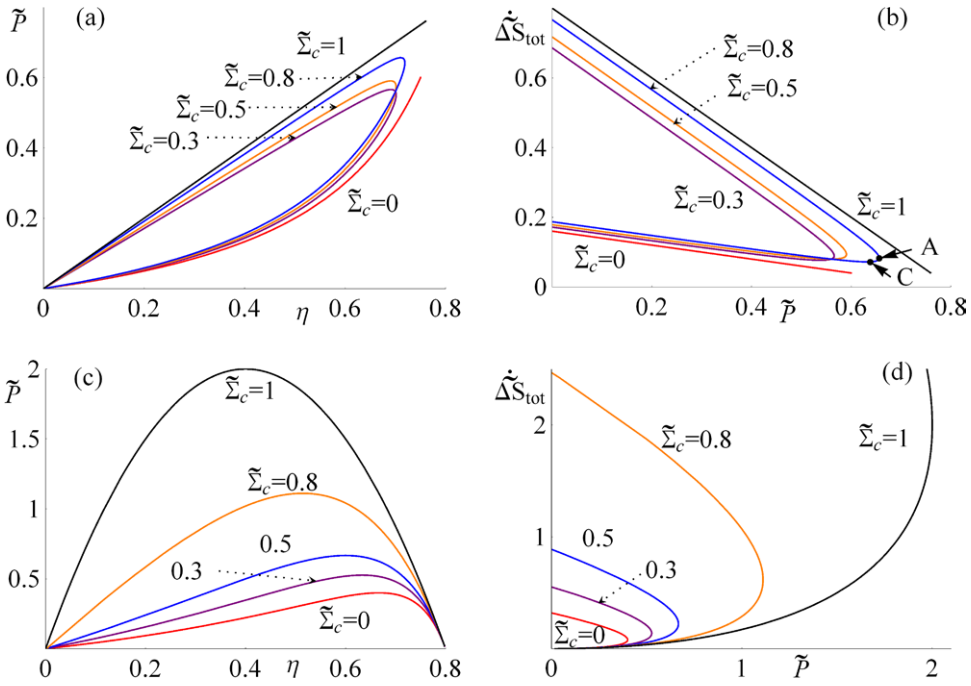

Figure 2. Parametric curves of η versus $\widetilde{P}$ and $\widetilde{P}$ versus $\dot{\widetilde{\Delta S}}_{\rm tot}$: (a), (b) for $\tilde{t}=5$, $\alpha\in(0,1)$ and (c), (d) for $\alpha=0.5$, $\tilde{t}\in(0,\infty)$. In all cases $\tau=0.2$, $\eta_C=0.8$. Note in (b) that the maxima of $\widetilde{P}$ (A) and the minima of $\dot{\widetilde{\Delta S}}_{\rm tot}$ (C) are not coincident.

J. Stat. Mech. (2016) 073202

$$\alpha_{\widetilde{P}_{\max}}(\tau,\widetilde{\Sigma}_{\rm c})=\frac{1}{1+\sqrt{\frac{1-\widetilde{\Sigma}_{\rm c}}{\tau\widetilde{\Sigma}_{\rm c}}}},\tag{12}$$

$$\tilde{t}_{\widetilde{P}_{\max}}(\tau,\widetilde{\Sigma}_{\rm c})=\frac{2}{1-\tau}\left(\sqrt{\tau\widetilde{\Sigma}_{\rm c}}+\sqrt{1-\widetilde{\Sigma}_{\rm c}}\right)^2.\tag{13}$$

From these values, the maximum power $\widetilde{P}_{\max}(\tau,\widetilde{\Sigma}_{\rm c})$ and the efficiency at maximum power $\eta_{\widetilde{P}_{\max}}(\tau,\widetilde{\Sigma}_{\rm c})$ are, respectively,

$$\widetilde{P}_{\max}(\tau,\widetilde{\Sigma}_{\rm c})=\frac{(\tau-1)^2}{4\tau\left[1+\widetilde{\Sigma}_{\rm c}(\tau-1)+2\sqrt{\widetilde{\Sigma}_{\rm c}\tau(1-\widetilde{\Sigma}_{\rm c})}\right]},\tag{14}$$

$$\eta_{\widetilde{P}_{\max}}(\tau,\widetilde{\Sigma}_{\rm c})=\frac{(1-\tau)\left[1+\sqrt{\frac{\tau\widetilde{\Sigma}_{\rm c}}{1-\widetilde{\Sigma}_{\rm c}}}\right]}{\left[1+\sqrt{\frac{\tau\widetilde{\Sigma}_{\rm c}}{1-\widetilde{\Sigma}_{\rm c}}}\right]^2+\tau\left(1-\frac{\widetilde{\Sigma}_{\rm c}}{1-\widetilde{\Sigma}_{\rm c}}\right)},\tag{15}$$

with the last equation being exactly the result reported by Esposito *et al* (see equation (8) in [2]).

In order to show a complete graphical view of the maximum power regime, the functions $\alpha_{\widetilde{P}_{\max}}(\tau,\widetilde{\Sigma}_{\rm c})$, $\tilde{t}_{\widetilde{P}_{\max}}(\tau,\widetilde{\Sigma}_{\rm c})$, $\eta_{\widetilde{P}_{\max}}(\tau,\widetilde{\Sigma}_{\rm c})$, $\widetilde{\Delta\dot{S}}_{\widetilde{P}_{\max}}(\tau,\widetilde{\Sigma}_{\rm c})$ together with maximum power $\widetilde{P}_{\max}(\tau,\widetilde{\Sigma}_{\rm c})$ are plotted in figure 3 for a typical $\tau=0.2$ value. As expected, the efficiency at maximum power monotonically ranges (see figure 3(d)) between a lower bound $\eta^{-}_{\widetilde{P}_{\max}}=\eta_C/2$ when all dissipations occur while the working system is in contact with the cold external bath ($\widetilde{\Sigma}_{\rm c}=\Sigma_{\rm c}/\Sigma_{\rm T}\to 1,\widetilde{\Sigma}_{\rm h}\to 0;\alpha\equiv t_{\rm c}/t\to 1$) and an upper bound $\eta^{+}_{\widetilde{P}_{\max}}=\eta_C/(2-\eta_C)$ when all dissipations are located in the hot external bath ($\widetilde{\Sigma}_{\rm h}=\Sigma_{\rm h}/\Sigma_{\rm T}\to 1,\Sigma_{\rm c}\to 0;1-\alpha\equiv t_{\rm h}/t\to 1$). The dissipation to the hot thermal bath has been interpreted in [39] as energy that can be re-utilized as input energy, thus allowing upper bounds for the efficiency. In between these lower and upper bounds, the Curzon–Ahlborn [56] value is recovered when dissipations are symmetrically distributed between the two external baths ($\eta^{\rm sym}_{\widetilde{P}_{\max}}\equiv 1-\sqrt{1-\eta_C},\widetilde{\Sigma}_{\rm c}=\widetilde{\Sigma}_{\rm h}=1/2$) but with a distribution of fractional contact times given by $\frac{\alpha}{1-\alpha}=\frac{t_{\rm c}}{t_{\rm h}}=\sqrt{\tau}$.

In spite of that the fractional contact times with external heat baths (figure 3(a)) and the maximum power efficiency (figure 3(d)) behave monotonically with $\widetilde{\Sigma}_{\rm c}$ we note that this is not the case for the corresponding total time cycle (figure 3(b)) nor the maximum power (figure 3(c)). It can be seen how $\tilde{t}_{\widetilde{P}_{\max}}(\tau,\widetilde{\Sigma}_{\rm c})$ shows a clear maximum value at $\widetilde{\Sigma}^{*}_{\rm c}\equiv\frac{\tau}{1+\tau}$ and, as a consequence, the maximum dimensionless power $\widetilde{P}_{\max}(\tau,\widetilde{\Sigma}_{\rm c})$ shows a non-monotonic behavior with a corresponding well defined minimum value (figure 3(c)) but accompanied by a monotonically increasing behavior of the entropy generation rate (figure 3(e)).

J. Stat. Mech. (2016) 073202

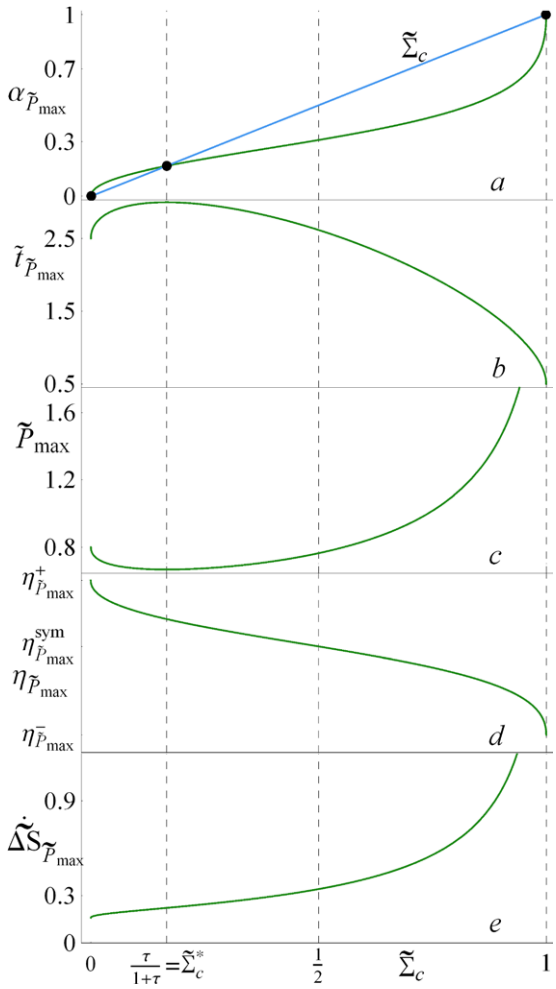

Figure 3. Maximum power regime: behavior of $\alpha_{\widetilde{P}_{max}}(\tau, \widetilde{\Sigma}_c)$, $\tilde{t}_{\widetilde{P}_{max}}(\tau, \widetilde{\Sigma}_c)$, $\widetilde{P}_{max}(\tau, \widetilde{\Sigma}_c)$, $\eta_{\widetilde{P}_{max}}(\tau, \widetilde{\Sigma}_c)$ and $\widetilde{\dot{\Delta}S}_{\widetilde{P}_{max}}(\tau, \widetilde{\Sigma}_c)$ with respect to $\widetilde{\Sigma}_c$ for a value of $\tau = 0.2$.

The value $\widetilde{\Sigma}_c^*$ has a notable feature since between 0 to $\widetilde{\Sigma}_c^*$ the contact time at the cold reservoir is greater than the dimensionless dissipation, while the opposite is true for the interval $\widetilde{\Sigma}_c^*$ to 1. This fact implies two distinct behaviors for the maximum power versus efficiency parametric curve. In figure 4 we have specified some relevant states of the $\widetilde{P}_{max}$ regime by their particular values of $\widetilde{\Sigma}_c$, $\tilde{t}$ and α. It is observed how the set of increasing efficiencies at maximum power allowed by the dissipation conditions (between $\eta_C/2$ and $\eta_C/(2-\eta_C)$) correspond to a maximum power behavior showing a well defined minimum value at $\tilde{t} = 2(2-\eta_c)/\eta_c = 3$ at $\eta_c = 0.8$ (see also figure 3). A valuable consequence is the feature of two possible states with the same maximum power but with very different associated efficiencies: one of them with the upper bound $\eta_c/(2-\eta_c)$ but the other with an optimized efficiency lower than the η_{CA} and greater than the lower bound $\eta_c/2$.

The existence of a simple relation between the three variables and the power is given by:

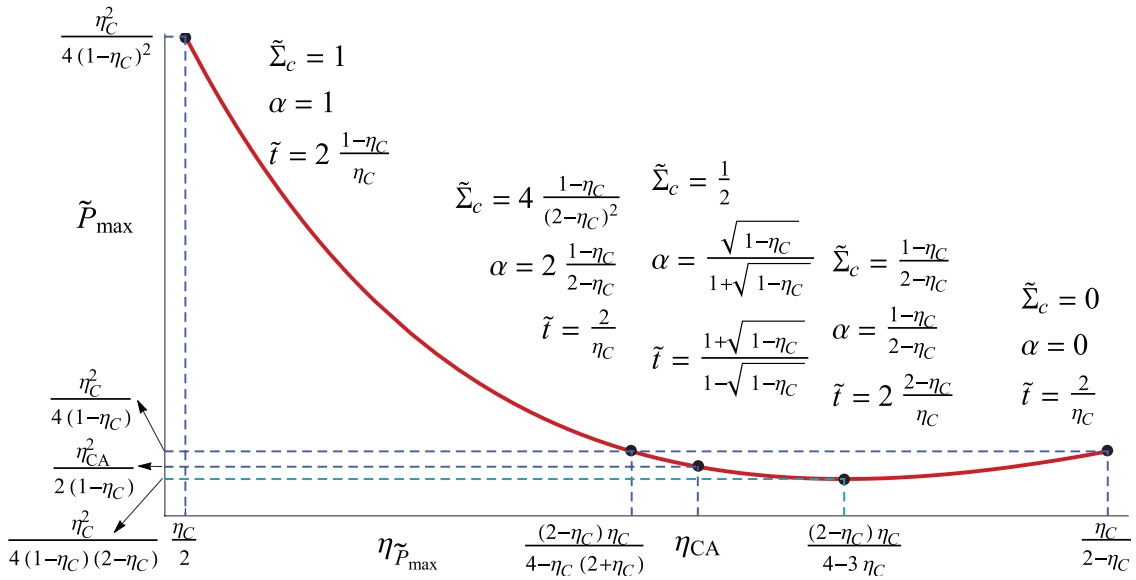

Figure 4. Parametric η-$\widetilde{P}$ plot at maximum power conditions. Some relevant points are labeled with the corresponding $\widetilde{\Sigma}_c$, α, and $\tilde{t}$ values and the associated values of the power and efficiency. Notice that all of them fulfill $\widetilde{P} = \frac{\widetilde{\Sigma}_c}{\alpha^2 \tilde{t}^2}$.

$$\widetilde{P}_{\max} = \frac{\widetilde{\Sigma}_c}{\alpha^2_{\widetilde{P}_{\max}}\, \tilde{t}^2_{\widetilde{P}_{\max}}}. \tag{16}$$

All cases depicted in figure 4 fulfill the above relation, and of special consideration is the limit $\widetilde{\Sigma}_c \to 0$

$$\lim_{\widetilde{\Sigma}_c \to 0} \frac{\widetilde{\Sigma}_c}{\alpha^2_{\widetilde{P}_{\max}}\, \tilde{t}^2_{\widetilde{P}_{\max}}} = \frac{\eta_C^2}{4} \lim_{\widetilde{\Sigma}_c \to 0} \Sigma_c \left(1 + \sqrt{\frac{1-\widetilde{\Sigma}_c}{(1-\eta_C)\widetilde{\Sigma}_c}}\right)^2 = \frac{\eta_C^2}{4(1-\eta_C)}, \tag{17}$$

which yields the labeled finite value of the maximum power at this point, as shown in figure 4.

3.1. Interpretation in an endoreversible Carnot-like framework

Despite the fact that there is no heat transfer dependence in the LD-model results, we saw above that LD-models allow for either loop-like parametric power versus efficiency curves or either open parabolic behaviors, depending on the constraints imposed on the total cycle time or the fractional contact times. This duality is clearly demonstrated by the maximum power regime as can be seen in figure 5 where each optimal state can be obtained from a closed or open curve.

Since the open form of the presented HE curves resembles the behavior found in a heat engine described by a Carnot-like endoreversible treatment, a closer inspection of the maximum power regime is appealing from this perspective in order to get additional physical insight from the comparison between two models with and without the specific

J. Stat. Mech. (2016) 073202

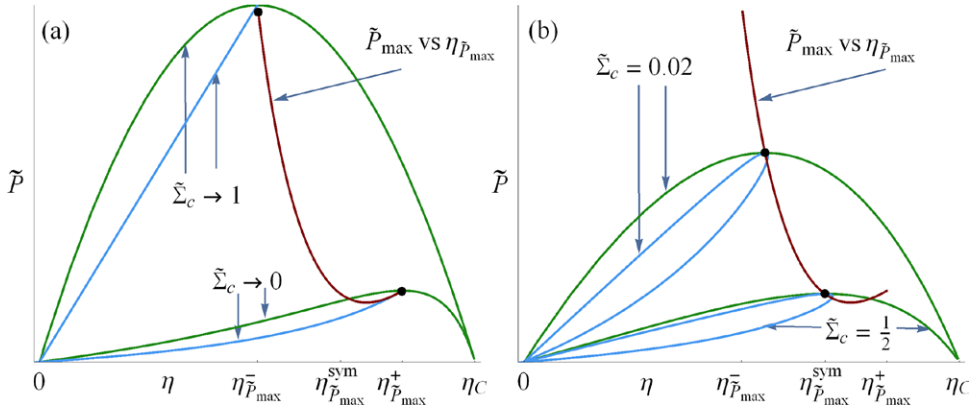

Figure 5. η versus $\widetilde{P}$ curves for the labeled $\widetilde{\Sigma}_c$ values. The open curves which resemble those obtained in endoreversible engines take values of characteristic times from 0 to 500. As $\tilde{t}$ increases the efficiency approaches η_C. Loops (in (b)) are bound by the open curves corresponding to $\widetilde{\Sigma}_c \to 0$ and $\widetilde{\Sigma}_c \to 1$ (see (a)). The $\widetilde{P}_{\max}$ state is depicted by the concave red curve.

consideration of heat transfer laws. We consider a generic endoreversible model (see figure 6) with generalized heat transfer fluxes given by [28–31]

$$\dot{Q}_{\mathrm{h}} = \sigma_{\mathrm{h}}(T_{\mathrm{h}}^{k} - T_{\mathrm{h}}'^{k}), \tag{18}$$

$$\dot{Q}_{\mathrm{c}} = \sigma_{\mathrm{c}}(T_{\mathrm{c}}'^{k} - T_{\mathrm{c}}^{k}), \tag{19}$$

where k is a real number specifying a concrete law (for instance, $k=1$ is the linear Newton law; $k=4$, the Stefan–Boltzmann radiation law; $k=-1$, the inverse law) and σ_{h} (σ_{c}) are the thermal conductances of the hot (cold) heat transferences, being positive for $k>0$ and negative otherwise. By applying the assumption of endoreversibility $\dot{Q}_{\mathrm{h}}\, t_{\mathrm{h}}/T_{\mathrm{h}}' = \dot{Q}_{\mathrm{c}}\, t_{\mathrm{c}}/T_{\mathrm{c}}'$ or equivalently $\eta = 1 - T_{\mathrm{c}}'/T_{\mathrm{h}}'$ to the inner cycle and optimizing with respect to the inner temperatures T_{h}' and T_{c}'. One can write the power in terms of the efficiency

$$P \equiv \frac{Q_{\mathrm{c}} + Q_{\mathrm{h}}}{t_{\mathrm{c}} + t_{\mathrm{h}}} = \sigma_{\mathrm{c}} T_{\mathrm{h}}^{k}\, \frac{\eta}{1-\eta}\, \frac{(1-\eta)^{k} - \tau^{k}}{\left(1 + \sqrt{\sigma_{\mathrm{ch}}(1-\eta)^{k-1}}\right)^{2}}. \tag{20}$$

From the above equation we obtain the results for the maximum power regime in terms of the exponent k and the ratio $\sigma_{\mathrm{ch}} = \sigma_{\mathrm{c}}/\sigma_{\mathrm{h}}$ which are depicted in figure 7. The extreme bounds of the LD-model and the CA-value are also shown. Two main features should be stressed from this figure:

(a) The CA-value can be obtained with different combinations of k and the asymmetry ratio σ_{ch} (for instance $\sigma_{\mathrm{ch}} \approx 10$ and the Stefan–Boltzmann heat transfer law $k=4$ or $\sigma_{\mathrm{ch}} = \tau$ and the inverse heat transfer law $k=-1$). However, only the linear heat transfer law ($k=1$) is compatible with the CA-value independently of any value of the ratio σ_{ch} and as such, it was deduced originally by Curzon and Ahlborn [56], although now is known that several equivalent results were published earlier [57, 58]. In other words, the CA value is not associated to any symmetry of the

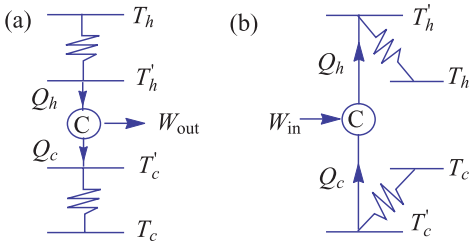

Figure 6. Sketch of an endoreversible Carnot-like heat engine (a) and a refrigerator (b).

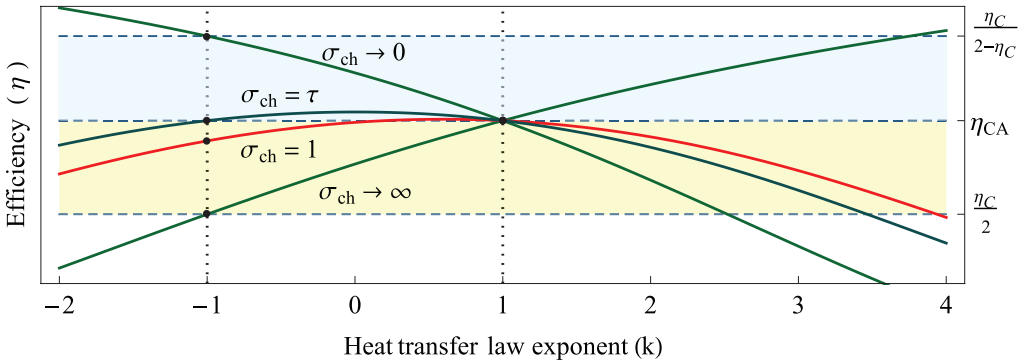

Figure 7. Maximum power efficiencies versus the exponent of the heat transfer law k in the endoreversible framework for the labeled values of the asymmetry σ_{ch} and comparison with the asymmetric and symmetric bounds in the LD-model. Only the inverse law $k=-1$ can reproduce all LD-results with appropriate σ_{ch} while the linear Newton law $k=1$ only reproduces the symmetric η_{CA} value for any value of σ_{ch}.

thermal conductances in the endoreversible models with a linear heat transfer law but it is linked to symmetric dissipations in the external heat baths in the LD-models where specific heat transfer laws do not play any role.

(b) Only the phenomenological heat transfer law ($k=-1$) with appropriate σ_{ch} allow the derivation of the all maximum power efficiency values obtained with the LD model. This fact should be remarked since the inverse law appears in a natural way in the linear irreversible thermodynamics frameworks as the appropriated thermodynamic law in the decomposition of entropy generation rate (see for instance [34]). At the sight of these coincidences may be suggestive to associate the same conceptual meaning to the ratios $\sigma_{ch}=\sigma_c/\sigma_h$ and Σ_c/Σ_h. By comparing the efficiencies at maximum power in equation (15) with the one obtained for $k=-1$ one can find that both are the same under the assumption that $\sigma_c/\sigma_h=\tau\widetilde{\Sigma}_c/\widetilde{\Sigma}_h=\tau\Sigma_c/\Sigma_h$

$$\eta_{P_{max},k=-1}=\frac{(1-\tau)\left[1+\sqrt{\sigma_{ch}}\right]}{1+\tau+2\sqrt{\sigma}_{ch}}=\frac{(1-\tau)\left[1+\sqrt{\frac{\tau\widetilde{\Sigma}_c}{1-\widetilde{\Sigma}_c}}\right]}{1+\tau+2\sqrt{\frac{\tau\widetilde{\Sigma}_c}{1-\widetilde{\Sigma}_c}}}=\eta_{\widetilde{P}_{max}}(\tau,\widetilde{\Sigma}_c). \quad (21)$$

Indeed, under limit asymmetric conditions $\sigma_{ch}=\sigma_c/\sigma_h\to 0$ ($\sigma_h\to\infty$) and $\Sigma_c/\Sigma_h\to 0$ ($\Sigma_h\to\infty$) both the inverse law and the LD-model give the upper bound $\eta_C/(2-\eta_C)$ and

under asymmetric conditions $\sigma_{ch} = \sigma_c/\sigma_h \to \infty$ ($\sigma_h \to 0$) and $\Sigma_c/\Sigma_h \to \infty$ ($\Sigma_h \to 0$) both models give the lower bound $\eta_C/2$. Also, the CA value comes in the LD model under the condition $\Sigma_c/\Sigma_h \to 1$ which corresponds in the endoreversible model with the inverse law giving the CA-value under the condition $\sigma_{ch} = \sigma_c/\sigma_h = \tau$. Notice that there exist a range of values of k in which the efficiency is located between the upper and lower bounds found in the LD model. Perhaps a detailed comparison between irreversible Carnot-like models with and without heat leak and LD-models with appropriate constraints could shed some light on this issue. This suggest that the rest of the cases containing values for the efficiency may not be reproduced by a LD description. Then, in the context of heat laws the results of LD are restricted to certain heat transfer mechanisms.

3.2. Interpretation in an exoreversible Carnot-like framework

For a stochastic brownian particle confined by an optic trap to perform a Carnot-like cycle, Schmield and Seifert [47] found that the maximum power efficiency can be written as $\eta_{ss} = \eta_C/(2 - \gamma_{ss}\eta_C)$, where γ_{ss} is a model-dependent parameter ranging between 0 and 1 which account for the irreversible actions on the isothermal processes. Apertet *et al* [39, 40] argued that η_{ss} apply to converter where all irreversibilities are restricted to internal processes while external coupling remain reversible keeping no differences between the internal temperatures of the working and external temperatures of the heat baths (the so-called exoreversible model). For a thermoelectric generator these authors found and physically explained a continuous transition between η_{ss} and η_{CA} by tuning the different irreversibilities on the system from internal to external losses.

Indeed η_{ss} reproduce all the values given by $\eta_{\widetilde{P}_{max}}$ in the LD model just fitting the model-dependent irreversibility distribution through the mesoscopic γ_{ss} and the macroscopic $\Sigma' s$.

For $\gamma_{ss} = 0$ and 1 the lower and upper bounds $\eta_C/2$ and $\eta_C/(2 - \eta_C)$ are obtained which correspond respectively with $\widetilde{\Sigma}_c = 1$, $\alpha = 1$ and $\widetilde{\Sigma}_h = 1$, $1 - \alpha = 1$. In between these two theoretical limits all values can be obtained by the appropriate election of the characteristic cycle time and its distribution in the contact time with the external baths together with the associated distributions of irreversibilities. In particular, the CA-efficiency result from symmetry in the dissipation constant $\Sigma_c = \Sigma_h$ but not in the corresponding contact times.

4. Results: refrigerator engines

As it has been the object of study in the proposal of a unified criteria of maximum power for HE and RE [14], an entirely similar study to that presented above for HE is possible for RE by replacing the power output $\widetilde{P}$ by the figure of merit $\widetilde{\chi}$, and the efficiency η by the COP ϵ. Thus, here we outline only the main results.

Representative 3D-graphs obtained for $\widetilde{\chi}$, ϵ and $\widetilde{\dot{\Delta S}}_{tot}$ for symmetric dissipation $\widetilde{\Sigma}_c = 0.5 = \widetilde{\Sigma}_h$ are plotted in figures 8(a) and (b). Open and closed behaviors of the curves with different constrains are also displayed in the HE case. Similar curves to those depicted in figure 2 can be obtained. Again, near but non-coincident maximum $\widetilde{\chi}$

J. Stat. Mech. (2016) 073202

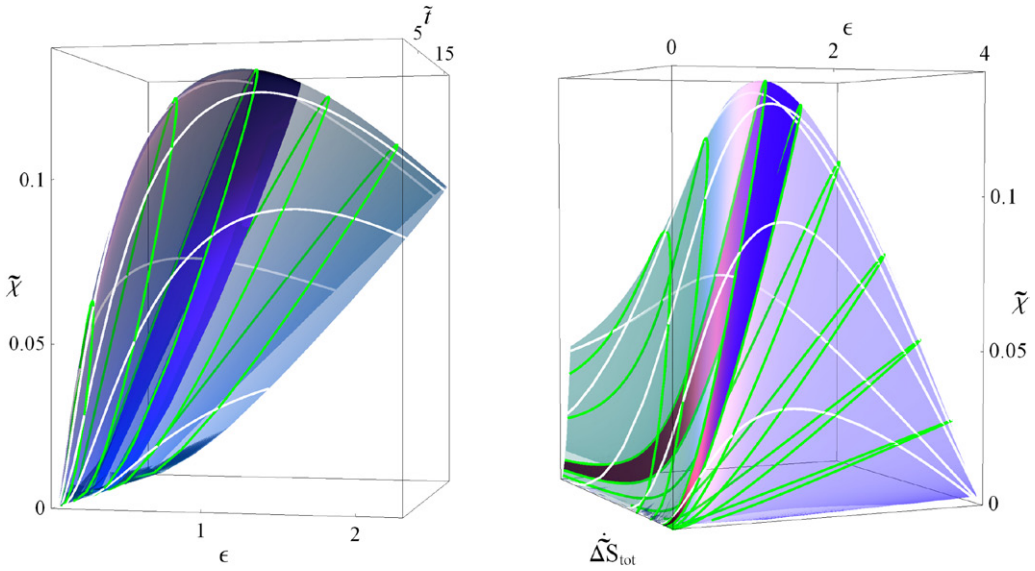

Figure 8. (a) Evolution of ϵ versus $\tilde{\chi}$ with respect to $\tilde{t}$. For $\tilde{t}$ = const. and $\alpha \in (0, 1)$ (green lines). For α = const. and $\tilde{t} \in (0, 20)$ (white lines). (b) Evolution of ϵ versus $\tilde{\chi}$ with respect to $\dot{\tilde{\Delta}}\tilde{S}_{\rm tot}$. $\tilde{t} \in (0, 20)$ and $\alpha \in (0, 1)$. In both cases $\tilde{t}$ fixed (green lines) corresponds to the characteristic loops of the real heat engines, meanwhile, for α fixed (white line) the endoreversible-like model behavior is found (see also figure 4).

and maximum COP states are clearly visible and confined by the monotonic behavior imposed by the limit values $\widetilde{\Sigma}_{\rm c} \to 1$ ($\widetilde{\Sigma}_{\rm h} \to 0$) and $\widetilde{\Sigma}_{\rm c} \to 0$ ($\widetilde{\Sigma}_{\rm h} \to 1$) or open curves when the fractional contact times are fixed.

The main characteristics of the criterion $\tilde{\chi}^{(\rm RE)}(\tau, \widetilde{\Sigma}_{\rm c}, \alpha, \tilde{t})$ were analyzed in [14]. Here we stress that it shows an absolute maxima on both α and $\tilde{t}$ (see figure 5(b) in [14]) in the same way to the power output in HE. Regrettably, the calculation of the absolute maximum is only achieved by numerical methods since no closed and general analytical expressions can be obtained for both α and $\tilde{t}$. The upper $\epsilon^{+}_{\tilde{\chi}_{\rm max}}$, lower $\epsilon^{-}_{\tilde{\chi}_{\rm max}}$, and symmetric $\epsilon^{\rm sym}_{\tilde{\chi}_{\rm max}}$ bounds obtained for the COP under maximum $\tilde{\chi}$ conditions read as [3, 4, 7]:

$$\epsilon^{+}_{\tilde{\chi}_{\rm max}} = \frac{\sqrt{9 + 8\epsilon_{\rm C}} - 3}{2}, \tag{22}$$

$$\epsilon^{-}_{\tilde{\chi}_{\rm max}} = 0, \tag{23}$$

and

$$\epsilon^{\rm sym}_{\tilde{\chi}_{\rm max}} = \sqrt{1 + \epsilon_{\rm C}} - 1 \equiv \epsilon_{\rm CA}. \tag{24}$$

The full characterization of the maximum χ-criteria is displayed in figure 9, where we have plotted $\alpha_{\tilde{\chi}_{\rm max}}(\tau, \widetilde{\Sigma}_{\rm c})$, $\tilde{t}_{\tilde{\chi}_{\rm max}}(\tau, \widetilde{\Sigma}_{\rm c})$, $\epsilon_{\tilde{\chi}_{\rm max}}(\tau, \widetilde{\Sigma}_{\rm c})$ and $\tilde{\chi}_{\rm max}(\tau, \widetilde{\Sigma}_{\rm c})$ for a typical $\tau = 0.8$ value in RE. We stress the notable similitude with the behavior obtained for maximum power in HE but now care should be taken because of the role played by $\widetilde{\Sigma}_{\rm c}$: the COP increases from its minimum, null value $\epsilon^{-}_{\tilde{\chi}_{\rm max}} = 0$ at $\widetilde{\Sigma}_{\rm c} = 0$ to the maximum $\epsilon^{+}_{\tilde{\chi}_{\rm max}}$ when

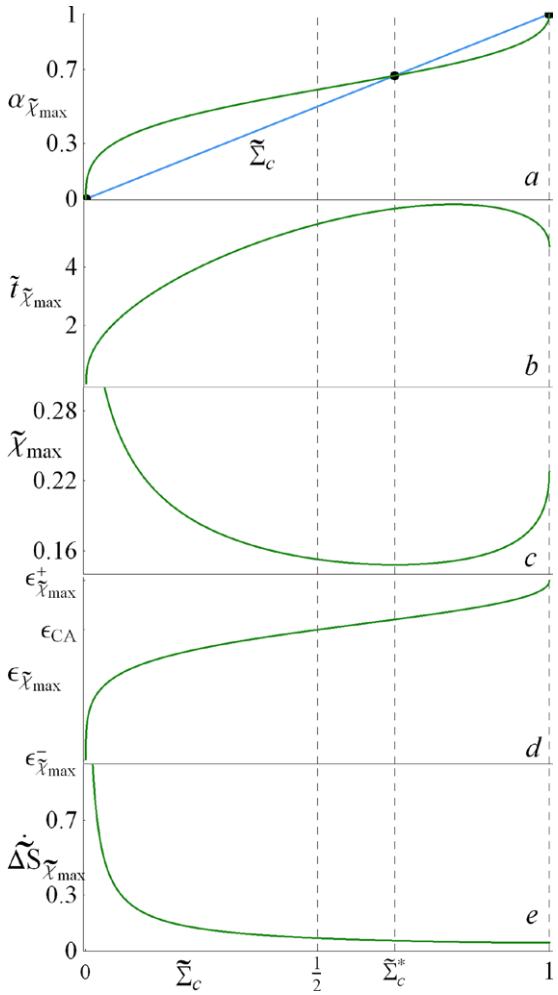

Figure 9. Maximum $\widetilde{\chi}$ regime: behavior of $\alpha_{\widetilde{\chi}_{\max}}(\tau, \widetilde{\Sigma}_c)$, $\tilde{t}_{\widetilde{\chi}_{\max}}(\tau, \widetilde{\Sigma}_c)$, $\widetilde{\chi}_{\max}(\tau, \widetilde{\Sigma}_c)$, $\eta_{\widetilde{\chi}_{\max}}(\tau, \widetilde{\Sigma}_c)$ and $\widetilde{\Delta S}_{\widetilde{\chi}_{\max}}(\tau, \widetilde{\Sigma}_c)$ with respect to Σ_c for a value of $\tau = 0.8$.

all dissipation are restricted in the cold thermal bath ($\widetilde{\Sigma}_c = 1$), opposite to what we observed in RE. Larger contact times with the hot reservoir produce more entropy (in characteristic units) and smaller values of ϵ. A straightforward consequence is that the parametric curve $\widetilde{\chi}_{\max}$ versus ϵ is qualitatively equal to $\widetilde{P}_{\max}$ versus η for HE, including the presence of a minimum value for $\widetilde{\chi}_{\max}$ near $\epsilon^{\text{sym}}_{\widetilde{\chi}_{\max}}$, at ϵ^*. As this is a numerical value, no analytical expression was found, this can be seen in figure 10.

The observed duality endoreversible-irreversible in HE is kept for RE in the LD-framework, as shown in figure 11 where each state $\widetilde{\chi}_{\max}(\tau, \Sigma_c)$ can be recovered either on an endoreversible or on an irreversible curve depending on the constraints imposed on the total cycle time or the fractional contact times.

4.1. Interpretation in an endoreversible Carnot-like framework

The endoreversible interpretation of the LD-refrigerators follow the same steps to the ones for HE in section 3.1. From figure 6(b), using generalized heat transfer fluxes given by

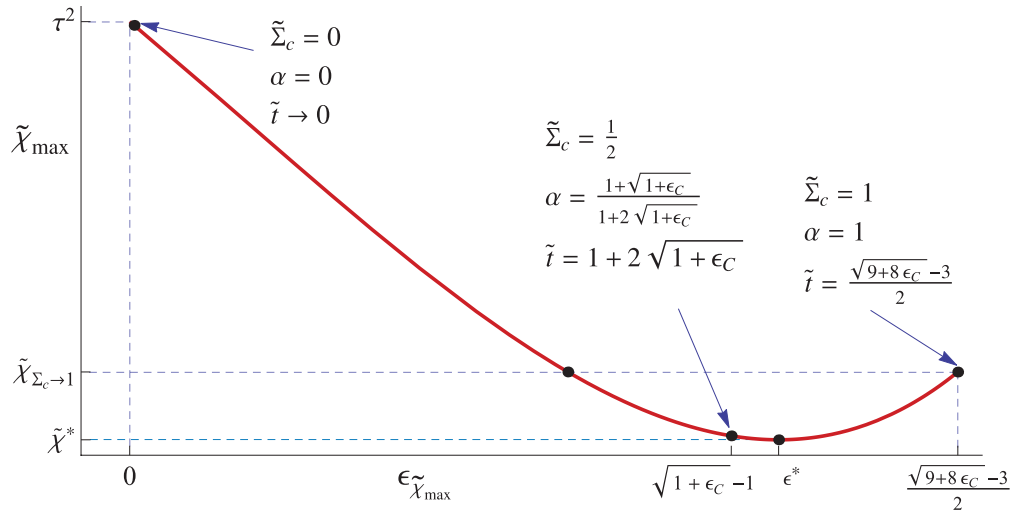

Figure 10. $\epsilon_{\tilde{\chi}_{\max}}$ versus $\tilde{\chi}_{\max}$ plot at maximum $\tilde{\chi}$ conditions. Some relevant points are labeled with the corresponding $\tilde{\Sigma}_c$, α, and $\tilde{t}$ values and the associated values of $\tilde{\chi}$ and COP.

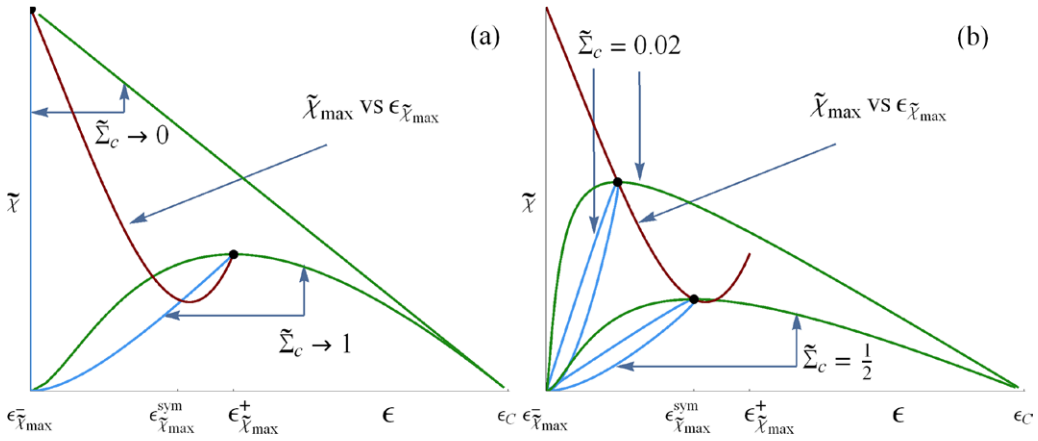

Figure 11. ϵ versus $\tilde{\chi}$ curves for the labeled values of $\tilde{\Sigma}_c$. The open curves take values of characteristic times from 0 to 500. As $\tilde{t}$ increases the efficiency approaches ϵ_C. Loops (in (b)) are bound by the open curves corresponding to $\tilde{\Sigma}_c \to 0$ and $\tilde{\Sigma}_c \to 1$ (see (a)). The $\tilde{\chi}_{\max}$ state is depicted by the concave curve (red curve in (a) and (b)).

$$\dot{Q}_h = \sigma_h(T'^k_h - T^k_h), \tag{25}$$

$$\dot{Q}_c = \sigma_c(T^k_c - T'^k_c), \tag{26}$$

and by applying the assumption of endoreversibility $\dot{Q}_h\, t_h/T'_h = \dot{Q}_c\, t_c/T'_c$ or equivalently $\epsilon = 1/(T'_h/T'_c - 1)$ one can write χ in terms of ϵ as

$$\chi = \sigma_c T^k_h\, \epsilon\, \frac{\tau^k - \left(\frac{\epsilon}{1+\epsilon}\right)^k}{\left(1 + \sqrt{\sigma_{ch}\left(\frac{\epsilon}{1+\epsilon}\right)^{k-1}}\right)^2}. \tag{27}$$

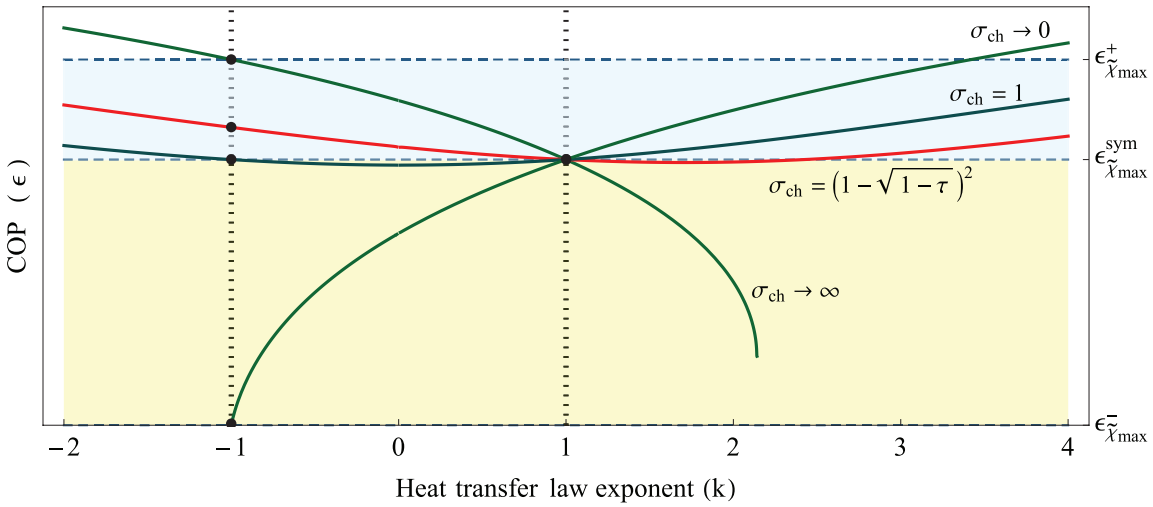

Figure 12. COP at $\widetilde{\chi}_{max}$ conditions with respect to the exponent of the heat transfer law k in the endoreversible framework for the labeled values of the asymmetry σ_{ch} and comparison with the asymmetric and symmetric bounds in the LD-model. Note again that only the inverse law $k = -1$ can reproduce all LD-results with appropriate σ_{ch} while the linear Newton law $k = 1$ only reproduces the symmetric ϵ_{CA} value for any value of σ_{ch}.

From the above equation it is easy to obtain the results for the maximum χ regime in terms of the exponent k and the ratio $\sigma_{ch} = \sigma_c/\sigma_h$. Notice the similarity of equations (20) and (27). The results for the COP at maximum χ are shown in figure 12 where the extreme bounds of the LD-model and the CA-value have been labeled. From figure 12 we note that:

(a) The ϵ_{CA}-value can be obtained with different combinations of k and of the asymmetry ratio but only the linear heat transfer law ($k = 1$) is compatible with the ϵ_{CA}-value independently of any value of the ratio σ_{ch}. The ϵ_{CA}-value (as occurs with η_{CA}) is not associated to any symmetry of the thermal conductances in the endoreversible models with a linear heat transfer law but it is linked to symmetric dissipations in the external heat baths in the LD-models where specific heat transfer laws do not play any role.

(b) Only the phenomenological heat transfer law ($k = -1$) with appropriate σ_{ch} allows the derivation of all the optimized maximum COP values obtained with the LD model. This could be a physical explanation why the inverse law appears in linear irreversible frameworks as a natural election of the thermodynamic force also in refrigerators.

5. Summary

In summary, we have presented a detailed analysis of a low dissipation heat engine stressing the role of the characteristics total cycle time (a point barely considered in

most reported papers), the contact times of the working system with the external heat baths and the symmetries/asymmetries associated to these contacts. The results reveal how different sources of irreversibility affect the main performance regimes. The results for the maximum power efficiency have been confronted with those obtained from endoreversible models (where specific heat transfer laws are needed) and with those obtained from exoreversible models (where no difference temperatures between the inner system and the external bath are assumed).

Under general arguments the observed universality of the maximum power efficiency of heat engines can be extended to the COP at maximum χ-conditions in RE. The validity of the inverse heat transfer law to generate all range of the maximum power efficiencies and of the COP under maximum χ conditions clarify its fundamental role in linear and non-linear irreversible frameworks. Since macroscopic constraints and symmetries reflect an underlying dynamic, the unified character of the results with the different models could be of some utility in the thermodynamic optimization of heat engines including stochastic, linear and non linear, and quantum frameworks [59–64].

Acknowledgment

J Gonzalez-Ayala acknowledge CONACYT-MÉXICO; A Calvo Hernández and JMMR acknowledge Ministerio de Economía y Competitividad of Spain under Grant ENE2013-40644R.

References

[1] Salamon P, Hoffmann K H, Schubert S and Berry R S 2001 What conditions make minimum entropy production equivalent to maximum power production? *J. Non-Equilib. Thermodyn.* **26** 73–83
[2] Esposito M, Kawai R, Lindenberg K and Van den Broeck C 2010 Efficiency at maximum power of low-dissipation Carnot engines *Phys. Rev. Lett.* **105** 150603
[3] de Tomás C, Calvo Hernández A and Roco J M M 2012 Optimal low symmetric dissipation Carnot engines and refrigerators *Phys. Rev.* E **85** 010104
[4] Wang Y, Li M, Tu Z C, Calvo Hernández A and Roco J M M 2012 Coefficient of performance at maximum figure of merit and its bounds for low-dissipation Carnot-like refrigerators *Phys. Rev.* E **86** 011127
[5] Hu Y, Wu F, Ma Y, He J, Wang J, Calvo Hernández A and Roco J M M 2013 Coefficient of performance for a low-dissipation Carnot-like refrigerator with nonadiabatic dissipation *Phys. Rev.* E **88** 062115
[6] de Tomás C, Roco J M M, Calvo Hernández A, Wang Y and Tu Z C 2013 Low-dissipation heat devices: unified trade-off optimization and bounds *Phys. Rev.* E **87** 012105
[7] Izumida Y, Okuda K, Calvo Hernández A and Roco J M M 2013 Coefficient of performance under optimized figure of merit in minimally nonlinear irreversible refrigerator *Europhys. Lett.* **101** 10005
[8] Guo J, Wang Y and Chen J 2012 General performance characteristics and parametric bounds of irreversible chemical engines *J. Appl. Phys.* **112** 103504
[9] Guo J, Wang J, Wang Y and Chen J 2013 Universal efficiency bounds of weak-dissipative thermodynamic cycles at the maximum power output *Phys. Rev.* E **87** 012133
[10] Guo J, Wang J, Wang Y and Chen J 2013 Efficiency of two-level weak dissipation quantum Carnot engines at the maximum power *J. Appl. Phys.* **113** 143510
[11] Holubec V and Artem R 2015 Efficiency at and near maximum power of low-dissipation heat engines *Phys. Rev.* E **92** 052125
[12] Wang Y and Tu Z C 2012 Bounds of efficiency at maximum power of low-dissipation Carnot engines *Europhys. Lett.* **98** 40001
[13] Van den Broeck C 2013 Efficiency at maximum power in the low-dissipation limit *Europhys. Lett.* **101** 10006
[14] Calvo Hernández A, Medina A and Roco J M M 2015 Time, entropy generation, and optimization in low-dissipation heat devices *New J. Phys.* **17** 075011

J. Stat. Mech. (2016) 073202

Calvo Hernández A, Medina A and Roco J M M 2016 *New J. Phys.* **18** 019501 (corrigendum)
[15] Sheng S, Yang P and Tu Z C 2014 Coefficient of performance at maximum χ-criterion for Feynman Ratchet as a refrigerator *Commun. Theor. Phys.* **62** 589–95
[16] Yuan Y, Wang R, He J, Ma Y and Wang J 2014 Coefficient of performance under maximum χ criterion in a two-level atomic system as a refrigerator *Phys. Rev.* E **90** 052151
[17] Liuzzo-Scorpo P, Correa L A, Schmidt R and Adesso G 2016 Thermodynamics of quantum feedback cooling *Entropy* **18** 48
[18] Correa L A, Palao J P and Alonso D 2015 Internal dissipation and heat leaks in quantum thermodynamic cycles *Phys. Rev.* E **92** 032136
[19] Correa L A, Palao J P, Adesso G and Alonso D 2014 Optimal performance of endoreversible quantum refrigerators *Phys. Rev.* E **90** 062124
[20] Correa L A, Palao J P, Alonso D and Adesso G 2014 Quantum-enhanced absorption refrigerators *Sci. Rep.* **4** 3949
[21] Correa L A, Palao J P, Adesso G and Alonso D 2013 Performance bound for quantum absorption refrigerators *Phys. Rev.* E **87** 042131
[22] Allahverdyan A E, Hovhannisyan K and Mahler G 2010 Optimal refrigerator *Phys. Rev.* E **81** 051129
[23] Long R and Liu W 2015 Performance of quantum Otto refrigerators with squeezing *Phys. Rev.* E **91** 062137
[24] Long R and Liu W 2015 Performance of micro two-level heat devices with prior information *Phys. Lett.* A **379** 1979–82
[25] Long R and Liu W 2015 Coefficient of performance and its bounds with the figure of merit of a general refrigerator *Phys. Scr.* **90** 025207
[26] Rana S, Pal P S, Saha A and Jayannavar A M 2015 Anomalous Brownian refrigerator *Physica* A **444** 783–98
[27] Abah O and Lutz E 2016 Optimal performance of a quantum Otto refrigerator *Europhys. Lett.* **113** 60002
[28] Yan Z and Chen J 1990 Optimal performance of a generalized Carnot cycle for another lineat heat transfer law *J. Chem. Phys.* **92** 1994–8
[29] Chen J 1994 The maximum power output and maximum efficiency on an irreversible Carnot heat engine *J. Phys. D: Appl. Phys.* **27** 1144–9
[30] Arias-Hernandez L A, de Parga G A and Angulo-Brown F 2003 On some nonendoreversible engine models with nonlinear heat transfer laws *Open Syst. Inf. Dyn.* **10** 351–75
[31] Chen L and Sun F 2004 *Advances in Finite-Time Thermodynamics: Analysis and Optimization* (New York: Nova Science)
[32] Gordon J M and Huleihil M 1992 General performance characteristics of real heat engines *J. Appl. Phys.* **72** 829–37
[33] Izumida Y, Okuda K, Roco J M M and Calvo Hernández A 2015 Heat devices in nonlinear irreversible thermodynamics *Phys. Rev.* E **91** 052140
[34] Van den Broeck C 2005 Thermodynamic efficiency at maximum power *Phys. Rev. Lett.* **95** 190602
[35] Schmiedl T and Seifert U 2007 Optimal finite-time processes in stochastic thermodynamics *Phys. Rev. Lett.* **98** 108301
[36] Esposito M, Linderberg K and Van den Broeck C 2009 Universality of efficiency at maximum power *Phys. Rev. Lett.* **102** 130602
[37] Izumida Y and Okuda K 2012 Efficiency at maximum power of minimally nonlinear irreversible heat engines *Europhys. Lett.* **97** 10004
[38] Gonzalez-Ayala J, Arias-Hernandez L A and Angulo-Brown F 2013 Connection between maximum-work and maximum-power thermal cycles *Phys. Rev.* E **88** 052142
[39] Apertet Y, Ouerdane H, Goupil C and Lecoeur Ph 2012 Irreversibilities and efficiency at maximum power of heat engines: the illustrative case of a thermoelectric generator *Phys. Rev.* E **85** 031116
[40] Ouerdane H, Apertet Y, Goupil C and Lecoeur Ph 2015 Continuity and boundary conditions in thermodynamics: from Carnot's efficiency to efficiencies at maximum power *Eur. Phys. J. Spec. Top.* **224** 839–62
[41] Izumida Y and Okuda K 2014 Work output and efficiency at maximum power of linear irreversible heat engines operating with a finite-sized heat source *Phys. Rev. Lett.* **112** 180603
[42] Wang Y 2014 Optimization in finite-reservoir finite-time thermodynamics *Phys. Rev.* E **90** 062140
[43] Gaveau B, Moreau M and Schulman L S 2010 Stochastic thermodynamics and sustainable efficiency in work production *Phys. Rev. Lett.* **105** 060601
[44] Aneja P, Katyayan H and Johal R S 2015 Optimal engine performance using inference for non-identical finite source and sink *Mod. Phys. Lett.* B **29** 1550217
[45] Johal R S 2015 Efficiency at optimal work from finite source and sink: a probabilistic perspective *J. Non-Equilib. Thermodyn.* **40** 1–12
[46] Arias-Hernandez L A, Angulo-Brown F and Paez-Hernandez R T 2008 First-order irreversible thermodynamic approach to a simple energy converter *Phys. Rev.* E **77** 011123

J. Stat. Mech. (2016) 073202

[47] Schmiedl T and Seifert U 2008 Efficiency of molecular motors at maximum power *Europhys. Lett.* **83** 30005
[48] Van den Broeck C, Kumar N and Lindenberg K 2012 Efficiency of isothermal molecular machines at maximum power *Phys. Rev. Lett.* **108** 210602
[49] Sánchez-Salas N, Chimal-Eguía J C, Ramírez-Moreno M A 2016 Optimum performance for energy transfer in a chemical reaction system *Physica* A **446** 224–33
[50] Wang R, Wang J, He J and Ma Y 2013 Efficiency at maximum power of a heat engine working with a two-level atomic system *Phys. Rev.* E **87** 042119
[51] Uzdin R and Kosloff R 2014 Universal features in the efficiency at maximum work of hot quantum Otto engines *Europhys. Lett.* **108** 40001
[52] Wu F, He J, Ma Y and Wang J 1990 Efficiency at maximum power of a quantum Otto engine: both within finite-time and irreversible thermodynamics *Phys. Rev.* E **90** 062134
[53] Jiménez de Cisneros B and Calvo-Hernández A 2008 Coupled heat devices in linear irreversible thermodynamics *Phys. Rev.* E **77** 041127
[54] Golubeva N and Imparato A 2012 Efficiency at maximum power of interacting molecular machines *Phys. Rev. Lett.* **109** 190602
Golubeva N and Imparato A 2013 *Phys. Rev. Lett.* **110** 149902 (erratum)
[55] Apertet Y, Ouerdane H, Goupil C and Lecoeur Ph 2012 Efficiency at maximum power of thermally coupled heat engines *Phys. Rev.* E **85** 041144
[56] Curzon F L and Ahlborn B 1975 Efficiency of a Carnot engine at maximum power output *Am. J. Phys.* **43** 22
[57] Calvo Hernandez A, Roco J M M, Medina A, Velasco S and Guzmán-Vargas L 2015 The maximum power efficiency 1-root tau: research, education, and bibliometric relevance *Eur. Phys. J. Spec. Top.* **224** 809–21
[58] Vaudrey A, Lanzetta F and Feidt M 2014 HB Reitlinger and the origins of the efficiency at maximum power formula for heat engines *J. Non-Equilib. Thermodyn.* **39** 199–203
[59] Sheng S and Tu Z C 2013 Universality of energy conversion efficiency for optimal tight-coupling heat engines and refrigerators *J. Phys. A: Math. Theor.* **46** 402001
[60] Sheng S Q and Tu Z C 2015 Constitutive relation for nonlinear response and universality of efficiency at maximum power for tight-coupling heat engines *Phys. Rev.* E **91** 022136
[61] Sheng S Q and Tu Z C 2015 Hidden symmetries and nonlinear constitutive relations for tight-coupling heat engines *New J. Phys.* **17** 045013
[62] Izumida Y and Okuda K 2015 Linear irreversible heat engines based on the local equilibrium assumptions *New J. Phys.* **17** 085011
[63] Cleuren B, Rutten B and Van den Broeck C 2015 Universality of efficiency at maximum power: macroscopic manifestation of microscopic constraints *Eur. Phys. J. Spec. Top.* **224** 879
[64] Wang Y 2016 Optimizing work output for finite-sized heat reservoirs: beyond linear response *Phys. Rev.* E **93** 012120

J. Stat. Mech. (2016) 073202